

Electronic Supplementary Information (ESI) for:

Single Molecule Magnet Behavior Observed in 1-D Dysprosium Chain with quasi- D_{5h} Symmetry

Xing-Cai Huang,^{a,b} Ming Zhang,^a Dayu Wu,^{*a} Dong Shao,^b Xin-Hua Zhao,^b Wei Huang^a and Xin-Yi Wang^{*b}

^a Jiangsu Key Laboratory of Advanced Catalytic Materials and Technology, Collaborative Innovation Center of Advanced Catalysis & Green Manufacturing, School of Petrochemical Engineering, Changzhou University, Changzhou, Jiangsu 213164, China;

^b State Key Laboratory of Coordination Chemistry, Collaborative Innovation Center of Advanced Microstructures, School of Chemistry and Chemical Engineering, Nanjing University, Nanjing, 210093, China

E-mail: wudy@cczu.edu.cn, wangxy66@nju.edu.cn

Table of contents

Experimental Section	S2
Physical Measurements	S4
X-ray data collection, structure solution and refinement for 1 and 2 .	S4
Figure S1. The powder XRD patterns for compound 1 and 2 .	S5
Figure S2. The crystal packing of 1 (a) and 2 (b).	S6
Table S1. Crystallographic data and structure refinement for 1 and 2 .	S7
Table S2. Crystallographic data and structure refinement for isostructural complexes 3–6 .	S8
Table S3. Selected Bond Distances (Å) and Angles (°) for 1 and 2 .	S8
Table S4. Continuous Shape Measures calculation for 1 and 2 .	S9
Table S5. Crystal field parameters for 1 and 2 fitted from $\chi_M T$ vs. T and M vs. H data.	S9
Table S6. Substates and corresponding energy levels 1 and 2 .	S10
Figure S3. Frequency dependence of the in-phase (χ') and out-of-phase (χ'') ac susceptibility for 1 at 2 K under the applied static field from 0 to 1500 Oe.	S10
Figure S4. Frequency dependence of the in-phase (χ') and out-of-phase (χ'') ac susceptibility for 2 at 2 K under the applied static field from 0 to 1500 Oe.	S11
Figure S5. Temperature dependence of the in-phase and out-of-phase ac susceptibility data for 1 under 1000 Oe dc field range from 1.8 to 10 K ($H_{ac}=1$ Oe).	S11
Figure S6. Temperature dependence of the in-phase and out-of-phase ac susceptibility data for 2 under 1000 Oe dc field range from 2 to 10 K ($H_{ac}=1$ Oe).	S12
Figure S7. The Cole-Cole plots at 1.8–4.0 K of 1 (a) and at 1.8–5.0 K of 2 (c) measured under 1000 Oe dc field ($H_{ac}=1$ Oe), and the red solid lines are the best fitting according to the generalized Debye model.	S12

Table S7. Relaxation Fitting Parameters from the Least-Square Fitting of the Cole-Cole plots of **1** according to the Generalized Debye Model. S12

Table S8. Relaxation Fitting Parameters from the Least-Square Fitting of the Cole-Cole plots of **2** according to the Generalized Debye Model. S13

Experimental Section

All preparations and manipulations were performed under aerobic conditions. The ligand H₂valdien was prepared according to a method described previously.^{S1} Preparation of **Na(PhO)₂PO₂**. (PhO)₂PO₂H (10 mmol, 0.25g) was added to the solution of NaOH (10 mmol, 0.4 g) in MeOH (20 mL), then the mixture was vigorously stirred for 2 hours at room temperature. The white solid (Na(PhO)₂PO₂) was obtained after evaporating the solution to dryness under reduced pressure without further purification for use directly.

[DyNa(valdien)Cl((PhO)₂PO₂)]_n (1). To a solution of H₂valdien (0.15 mmol, 55 mg), Et₃N (0.30 mmol, 41.8 μL) in MeOH (3 mL) was added a MeOH solution (2 mL) of DyCl₃·6H₂O (0.15 mmol, 57 mg). The solution was stirred for 3 min, and then a MeOH solution (2 mL) of Na(PhO)₂PO₂ (0.3 mmol, 81 mg) was added to the mixture. The resulting clear yellow solution was stirred briefly and filtered. The yellow block crystals suitable for X-ray diffraction studies were obtained by slow diffusion of isopropyl ether vapour into the yellow solution after 3 days. Yield: *ca.* 45%. Elemental analysis (%) calculated for C₃₂H₃₃ClDyN₃NaO₈P: C, 45.78; H, 3.96; N, 5.01. Found: C, 45.70; H, 3.85; N, 4.96. IR (KBr, cm⁻¹): 3439(w), 3200(w), 2916(w), 1626(vs), 1454(s), 1218(s), 1097(s), 899(m) and 741(m).

[Dy(valdien)((PhO)₂PO₂)]_n (2). To a solution of H₂valdien (0.15 mmol, 55 mg), Et₃N (0.30 mmol, 41.8 μL) and DyCl₃·6H₂O (0.15 mmol, 57 mg) in DMF/MeOH (5 mL, v/v = 1/4) was added a DMF/MeOH (5 mL, v/v = 1/4) solution of (PhO)₂PO₂H (0.3 mmol, 112 mg) and Et₃N (0.45 mmol, 62.8 μL). The resulting clear yellow solution was stirred briefly and filtered. The yellow block crystals suitable for X-ray diffraction studies were obtained by slow diffusion of isopropyl ether vapour into the yellow solution after 3 days. Yield: *ca.* 30%. Elemental analysis (%) calculated for C₃₂H₃₃DyN₃O₈P: C, 49.21; H, 4.26; N, 5.38. Found: C, 49.11; H, 4.18; N, 5.22. IR (KBr, cm⁻¹): 3432(w), 3231(w), 2927(w), 1626(vs), 1449(m), 1225(vs), 1108(m),

939(m), 859(w), and 739(m).

[GdNa(valdien)Cl((PhO)₂PO₂)_n (3). The same procedure was used to synthesize **1** except that DyCl₃·6H₂O was used in place of GdCl₃·6H₂O. Yield: *ca.* 53%. Elemental analysis (%) calculated for C₃₂H₃₃ClGdN₃NaO₈P: C, 46.07; H, 3.99; N, 5.04. Found: C, 46.14; H, 3.87; N, 5.18. IR (KBr, cm⁻¹): 3435(w), 3200(w), 2877(w), 1623(vs), 1450(m), 1220(vs), 1080(m), 901(m), 858(w), and 737(m).

[TbNa(valdien)Cl((PhO)₂PO₂)_n (4). The same procedure was used to synthesize **1** except that DyCl₃·6H₂O was used in place of TbCl₃·6H₂O. Yield: *ca.* 48%. Elemental analysis (%) calculated for C₃₂H₃₃ClTbN₃NaO₈P: C, 45.98; H, 3.99; N, 5.03. Found: C, 45.76; H, 4.03; N, 5.11. IR (KBr, cm⁻¹): 3445(w), 3201(w), 2868(w), 1625(vs), 1446(m), 1213(vs), 1096(m), 901(m), 859(w), and 739(m).

[HoNa(valdien)Cl((PhO)₂PO₂)_n (5). The same procedure was used to synthesize **1** except that DyCl₃·6H₂O was used in place of HoCl₃·6H₂O. Yield: *ca.* 42%. Elemental analysis (%) calculated for C₃₂H₃₃ClHoN₃NaO₈P: C, 45.65; H, 3.95; N, 4.99. Found: C, 45.77; H, 4.06; N, 4.88. IR (KBr, cm⁻¹): 3430(w), 3200(w), 2862(w), 1623(vs), 1449(m), 1220(vs), 1095(m), 911(m), 852(w), and 737(m).

[Ho(valdien)((PhO)₂PO₂)_n (6). The same procedure was used to synthesize **2** except that DyCl₃·6H₂O was used in place of HoCl₃·6H₂O. Yield: *ca.* 25%. Elemental analysis (%) calculated for C₃₂H₃₃HoN₃O₈P: C, 49.05; H, 4.25; N, 5.36. Found: C, 48.89; H, 4.28; N, 5.22. IR (KBr, cm⁻¹): 3440(w), 3236(w), 2857(w), 1618(vs), 1458(m), 1215(vs), 1110(m), 931(m), 854(w), and 732(m).

Physical Measurements

Elemental analyses were carried out a Vario EL II Elementar. Infrared spectra were obtained on a Thermo Scientific Nicolet IS5 spectrometer. Powder X-ray diffraction (PXRD) were recorded at 298 K on a RINT2000 vertical goniometer with Cu K α X-ray source (operated at 40kV and 100 mA). Magnetic measurements were performed on powdered samples with Quantum Design SQUID VSM magnetometers with field up to 7 T. All data were corrected for diamagnetism and the sample holder and of the constituent atoms using Pascal's constants.^{S2}

X-ray data collection, structure solution and refinement for 1–6

The X-ray data of **1–6** were collected on a Bruker APEX II with a CCD area detector ($\text{MoK}\alpha$ radiation, $\lambda = 0.71073 \text{ \AA}$). The APEX II program was used to determine the unit cell parameters and for data collection. The data were integrated using SAINT^{S3} and SADABS.^{S4} The structures for two compounds were solved by direct methods and refined by full-matrix least-squares based on F^2 using the SHELXTL program.^{S5} All the non-hydrogen atoms were refined anisotropically. Hydrogen atoms of the organic ligands were refined as riding on the corresponding non-hydrogen atoms. Additional details of the data collections and structural refinement parameters are provided in Table S1 (**1** and **2**) and Table S2 (**3–6**). Selected bond lengths and bond angles for **1** and **2** are listed in Table S3. CCDC- 1415417 (**1**), CCDC- 1415418 (**2**), CCDC-1432155 (**3**), CCDC-1432156 (**4**), CCDC-1432157 (**5**) and CCDC-1432220 (**6**) contain the supplementary crystallographic data for this paper. These data can be obtained free of charge from The Cambridge Crystallographic Data Centre via www.ccdc.cam.ac.uk/data_request/cif.

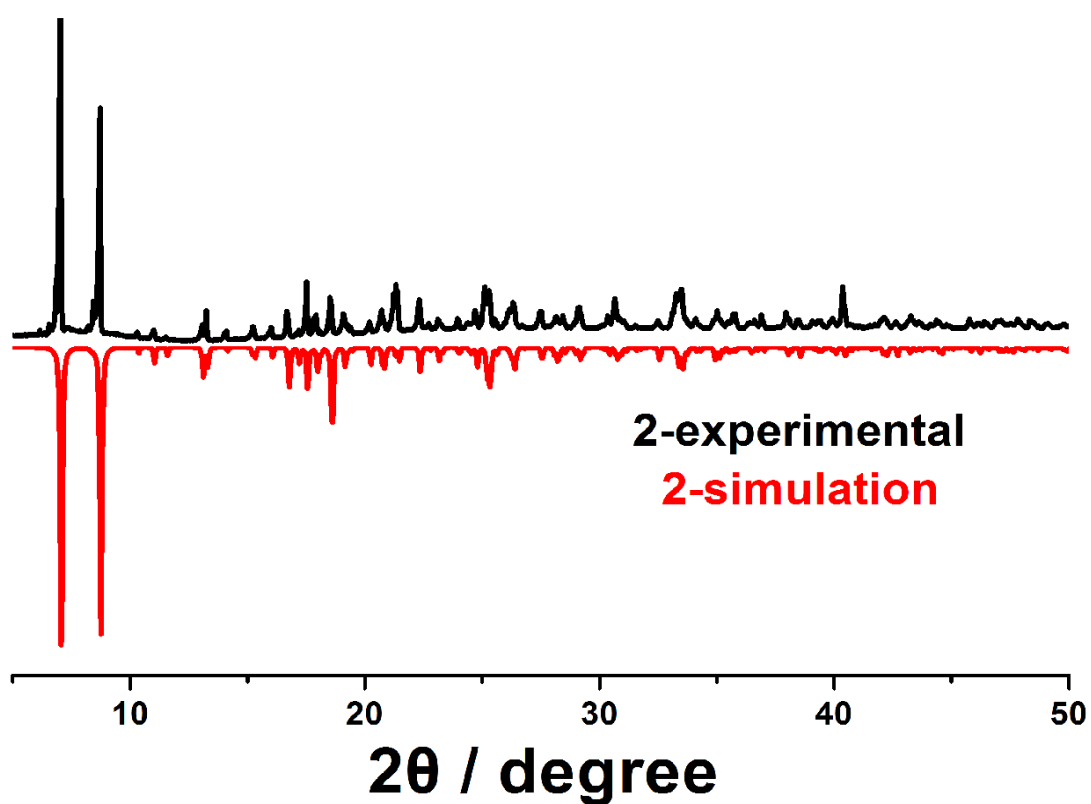
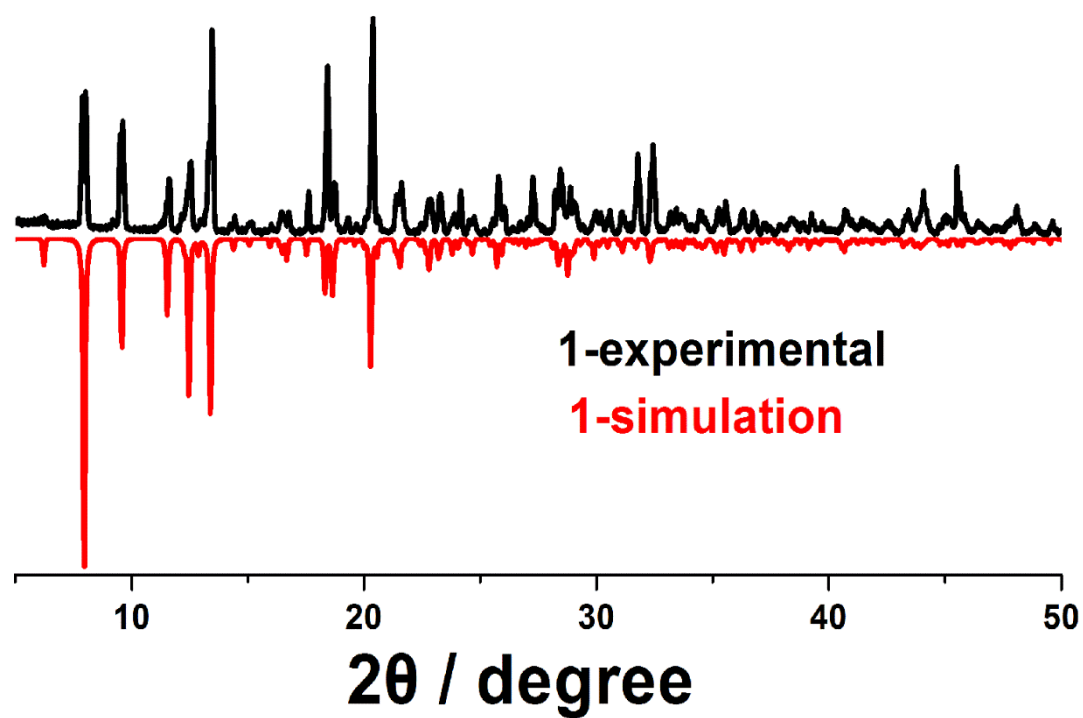


Figure S1. The powder XRD patterns for compound 1 and 2. The pattern simulated from the single crystal data of compound 1 and 2 are also given.

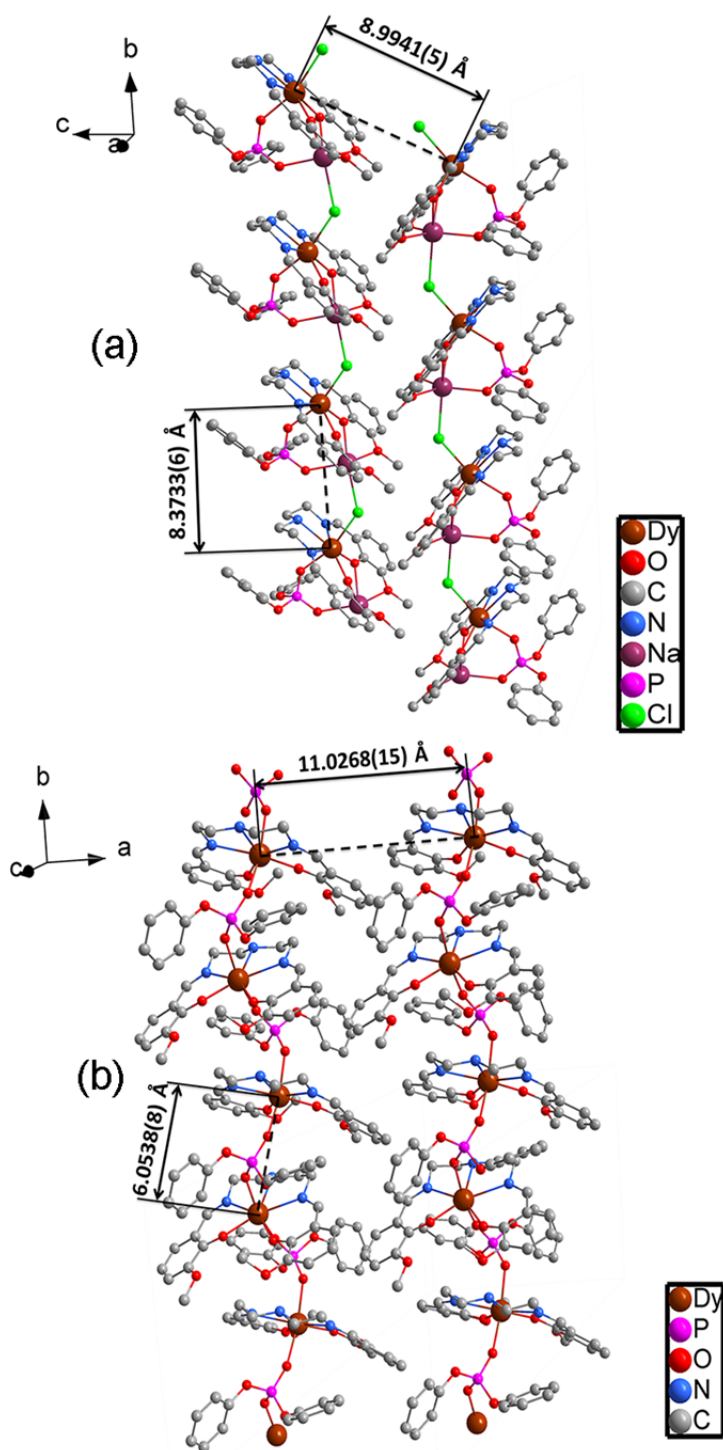


Figure S2. The crystal packing of **1** (a) and **2** (b). The shortest distances of Dy···Dy in the chain for **1** (a) and **2** (b) are 8.3733(6) and 6.0538(8) Å, respectively. And the nearest distances of Dy···Dy between the chain for **1** (a) and **2** (b) are 8.9941(5) and 11.0268(15) Å, respectively.

Table S1. Crystallographic data and structure refinement for **1** and **2**.

complex	1	2
Formula	DyNaC ₃₂ H ₃₃ N ₃ O ₈ ClP	DyC ₃₂ H ₃₃ N ₃ O ₈ P
<i>Mr</i> [g mol ⁻¹]	839.52	781.08
CCDC number	1415417	1415418
Crystal size [mm ³]	0.54×0.50×0.48	0.24×0.21×0.16
Crystal system	Orthorhombic	Monoclinic
Space group	<i>P bca</i>	<i>P 2₁/c</i>
<i>a</i> [Å]	22.2015(14)	11.0268(15)
<i>b</i> [Å]	8.3733(5)	11.6462(16)
<i>c</i> [Å]	36.918(2)	27.317(3)
α [°]	90	90
β [°]	90	113.808(4)
γ [°]	90	90
<i>V</i> [Å ³]	6863.0(7)	3209.5(7)
<i>Z</i>	8	4
<i>T</i> , K	293(2)	293(2)
ρ_{calcd} [g cm ⁻³]	1.625	1.616
μ (Mo– <i>K</i> α) [mm ⁻¹]	2.368	2.432
<i>F</i> (000)	3352	1564
θ range [°]	1.83 – 27.63	1.93 – 27.62
Refl. collected / unique	43751 / 7952	20718 / 7318
R(int)	0.0311	0.0537
<i>T</i> _{max} / <i>T</i> _{min}	0.3961 / 0.3613	0.6969 / 0.5929
Data/restraints/parameters	7952 / 0 / 430	7318 / 0 / 408
<i>R</i> ₁ ^a / <i>wR</i> ₂ ^b (<i>I</i> > 2 σ (<i>I</i>))	0.0403 / 0.0792	0.0390 / 0.0808
<i>R</i> ₁ / <i>wR</i> ₂ (all data)	0.0496 / 0.0823	0.0678 / 0.1016
GOF on <i>F</i> ²	1.239	1.032
Max/min [e Å ⁻³]	1.391 / -1.942	0.725 / -0.953

$$^a R_1 = \sum ||F_o| - |F_c|| / \sum |F_o|. \quad ^b wR_2 = \{ \sum [w(F_o^2 - F_c^2)^2] / \sum [w(F_o^2)^2] \}^{1/2}$$

Table S2. Crystallographic data and structure refinement for isostructural complexes **3–6**.

complex	3	4	5	6
Formula	GdNaC ₃₂ H ₃₃ ClN ₃ O ₈ P	TbNaC ₃₂ H ₃₃ N ₃ O ₈ CIP	HoNaC ₃₂ H ₃₃ NO ₈ CIP	HoC ₃₂ H ₃₃ N ₃ O ₈ P
<i>Mr</i> [g mol ⁻¹]	834.27	835.94	841.95	783.51
CCDC number	1432155	1432156	1432157	1432220
Crystal size [mm ³]	0.32 × 0.31 × 0.28	0.54 × 0.46 × 0.35	0.41 × 0.22 × 0.10	0.24 × 0.20 × 0.14
Crystal system	Orthorhombic	Orthorhombic	Orthorhombic	Monoclinic
Space group	<i>P bca</i>	<i>P bca</i>	<i>P bca</i>	<i>P 2₁/c</i>
<i>a</i> [Å]	22.267(3)	22.2076(17)	22.220(4)	10.990(2)
<i>b</i> [Å]	8.4192(13)	8.4021(7)	8.3683(16)	11.579(2)
<i>c</i> [Å]	36.839(6) A	36.877(3)	36.890(7)	27.216(5)
α [°]	90.00	90.00	90.00	90.00
β [°]	90.00	90.00	90.00	113.817(6)
γ [°]	90.00	90.00	90.00	90.00
<i>V</i> [Å ³]	6906.3(18)	6880.9(10)	6859(2)	3168.4(10)
<i>Z</i>	8	8	8	4
<i>T</i> , K	293(2)	293(2)	293(2)	293(2)
ρ_{calcd} [g cm ⁻³]	1.605	1.614	1.631	1.643
μ (Mo- <i>K</i> α) [mm ⁻¹]	2.110	2.245	2.497	2.603
<i>F</i> (000)	3336	3344	3360	1568
θ range [°]	2.14 – 27.47	2.14 – 27.45	1.43 – 27.47	1.94 – 26.00
Refl. collected / unique	42211 / 7834	41969 / 7836	42754 / 7821	33248 / 5992
R(int)	0.0438	0.0575	0.0726	0.0367
<i>T</i> _{max} / <i>T</i> _{min}	0.5896 / 0.5517	0.5071 / 0.3769	0.7883 / 0.4275	0.7120 / 0.5739
Data/restraints/ parameters	7834 / 0 / 426	7836 / 0 / 426	7821 / 0 / 426	6206 / 144 / 408
<i>R</i> ₁ ^a / <i>wR</i> ₂ ^b (<i>I</i> > 2 σ (<i>I</i>))	0.0415 / 0.0738	0.0425 / 0.0777	0.0367 / 0.0852	0.0357 / 0.0744
<i>R</i> ₁ / <i>wR</i> ₂ (all data)	0.0561 / 0.0778	0.0651 / 0.0842	0.0722 / 0.1134	0.0480 / 0.0798
GOF on <i>F</i> ²	1.173	1.077	1.014	1.064
Max/min [e Å ⁻³]	0.821 / -2.064	1.045 / -1.489	0.532 / -0.697	1.460 / -1.869

$$^a R_1 = \sum ||F_o| - |F_c|| / \sum |F_o|. \quad ^b wR_2 = \{ \sum [w(F_o^2 - F_c^2)^2] / \sum [w(F_o^2)^2] \}^{1/2}$$

Table S3. Selected Bond Lengths (Å) and Angles (°) for **1** and **2**.

1					
Dy1-O1	2.211(3)	O1-Dy1-O5	89.49(10)	O3-Dy1-N3	72.36(11)
Dy1-O3	2.232(3)	O3-Dy1-O5	89.06(10)	O5-Dy1-N3	85.95(11)
Dy1-O5	2.294(3)	O1-Dy1-N2	140.60(11)	N2-Dy1-N3	68.06(12)
Dy1-N2	2.493(3)	O3-Dy1-N2	139.34(11)	N1-Dy1-N3	136.42(12)
Dy1-N1	2.515(4)	O5-Dy1-N2	79.41(10)	O1-Dy1-Cl1	103.71(8)
Dy1-N3	2.530(4)	O1-Dy1-N1	73.31(11)	O3-Dy1-Cl1	104.32(8)

Dy1-Cl1	2.6390(12)	O3-Dy1-N1	150.16(11)	O5-Dy1-Cl1	162.87(7)
Dy1-Na1	3.6270(16)	O5-Dy1-N1	86.20(11)	N2-Dy1-Cl1	83.46(8)
		N2-Dy1-N1	68.36(12)	N1-Dy1-Cl1	87.21(9)
O1-Dy1-O3	77.21(10)	O1-Dy1-N3	149.28(11)	N3-Dy1-Cl1	87.98(9)
O1-Dy1-Na1	40.57(8)	O3-Dy1-Na1	40.83(8)	O5-Dy1-Na1	75.05(7)
N2-Dy1-Na1	154.46(8)	N1-Dy1-Na1	109.82(9)	N3-Dy1-Na1	109.30(9)
Cl1-Dy1-Na1	122.08(4)				
2					
Dy1-O1	2.197(3)	O1-Dy1-O6 ^a	99.69(13)	N3-Dy1-N2	66.78(14)
Dy1-O3	2.202(3)	O3-Dy1-O6 ^a	91.83(13)	O1-Dy1-N1	72.52(14)
Dy1-O5	2.261(3)	O5-Dy1-O6 ^a	163.10(13)	O3-Dy1-N1	153.81(14)
Dy1-O6 ^a	2.279(3)	O1-Dy1-N3	152.56(14)	O5-Dy1-N1	86.58(13)
Dy1-N3	2.532(4)	O3-Dy1-N3	71.56(14)	O6 ^a -Dy1-N1	85.61(13)
Dy1-N2	2.533(4)	O5-Dy1-N3	85.28(13)	N3-Dy1-N1	134.35(15)
Dy1-N1	2.536(4)	O6 ^a -Dy1-N3	89.50(13)	N2-Dy1-N1	67.59(14)
		O1-Dy1-N2	139.87(14)	O3-Dy1-O5	101.69(13)
O1-Dy1-O5	92.21(13)	O3-Dy1-N2	137.85(13)	O6 ^a -Dy1-N2	81.83(13)
O1-Dy1-O3	82.28(13)	O5-Dy1-N2	81.33(14)		

Symmetry transformations used to generate equivalent atoms: ^a x, y-1, z

Table S4. Continuous Shape Measures calculation for **1** and **2**.

Structure [ML7]	HP-7	HPY-7	PBPY-7	COC-7	CTPR-7	JPBPY-7	JETPY-7
1	33.490	25.169	0.775	8.133	6.113	4.712	23.157
2	33.887	24.701	0.496	6.561	4.970	3.056	23.699

HP-7 1 D7h Heptagon; HPY-7 2 C6v Hexagonal pyramid;

PBPY-7 3 D5h Pentagonal bipyramid; COC-7 4 C3v Capped octahedron;

CTPR-7 5 C2v Capped trigonal prism; JPBPY-7 6 D5h Johnson pentagonal bipyramid J13;

JETPY-7 7 C3v Johnson elongated triangular pyramid J7

Table S5. Crystal field parameters and anisotropy g-factors for **1** and **2** fitted from $\chi_M T$ vs. T and M vs. H data.

	1	2
B_2^0	-21.203	-17.096
B_4^0	-36.539	-26.606
B_6^0	56.616	55.275
g_x	1.320	1.927
g_y	1.373	0.128
g_z	1.189	1.342
Residual	0.038	0.041

Table S6. The substates and corresponding energy levels **1** and **2**.

1		2	
$ m_j\rangle$	$E(\text{cm}^{-1})$	$ m_j\rangle$	$E(\text{cm}^{-1})$
$\pm 13/2$	0	$\pm 13/2$	0
$\pm 11/2$	41.63	$\pm 11/2$	45.65
$\pm 1/2$	53.49	$\pm 1/2$	46.09
$\pm 3/2$	87.11	$\pm 3/2$	80.71
$\pm 9/2$	119.8	$\pm 9/2$	122.0
$\pm 5/2$	131.8	$\pm 5/2$	127.5
$\pm 7/2$	152.3	$\pm 7/2$	151.0
$\pm 15/2$	200.7	$\pm 15/2$	183.3

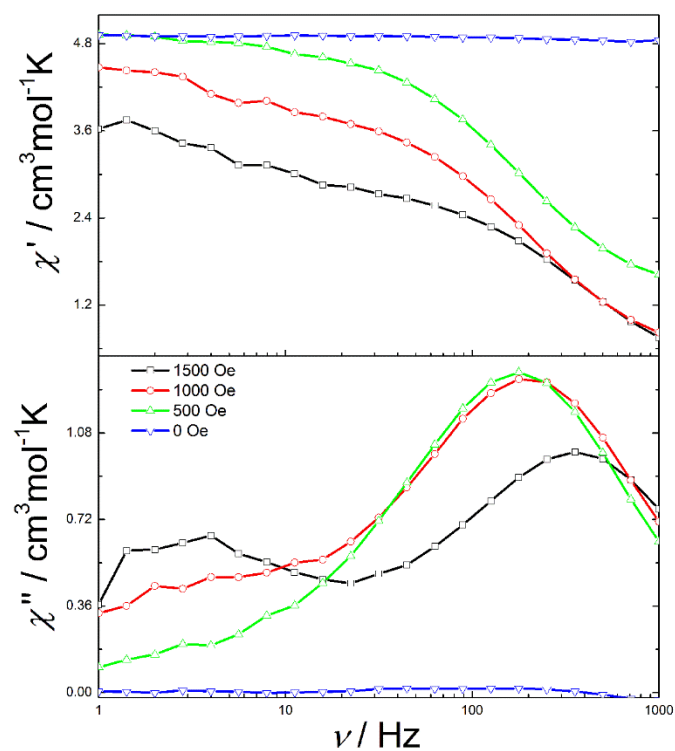


Figure S3. Frequency dependence of the in-phase (χ') and out-of-phase (χ'') ac susceptibility for **1** at 2 K under the applied static field from 0 to 1500 Oe. The solid lines are a guide for the eye.

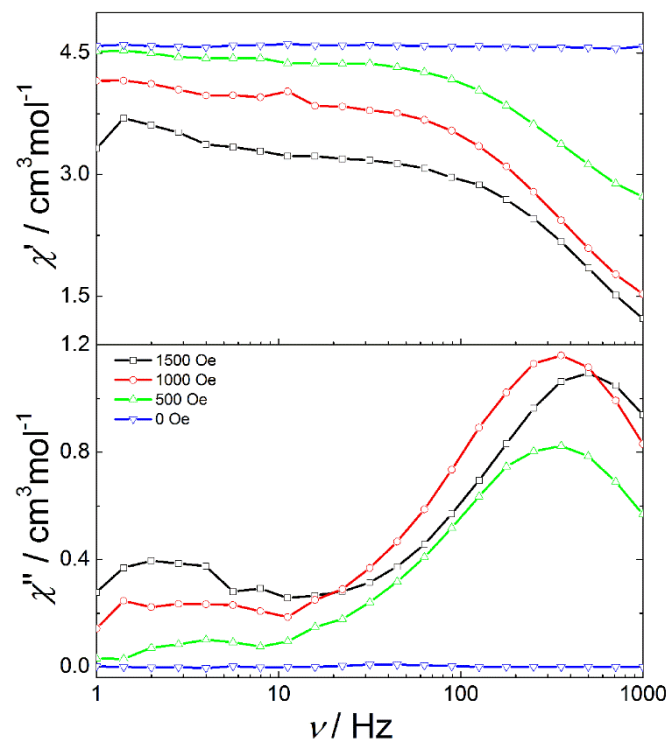


Figure S4. Frequency dependence of the in-phase (χ') and out-of-phase (χ'') ac susceptibility for **2** at 2 K under the applied static field from 0 to 1500 Oe. The solid lines are a guide for the eye.

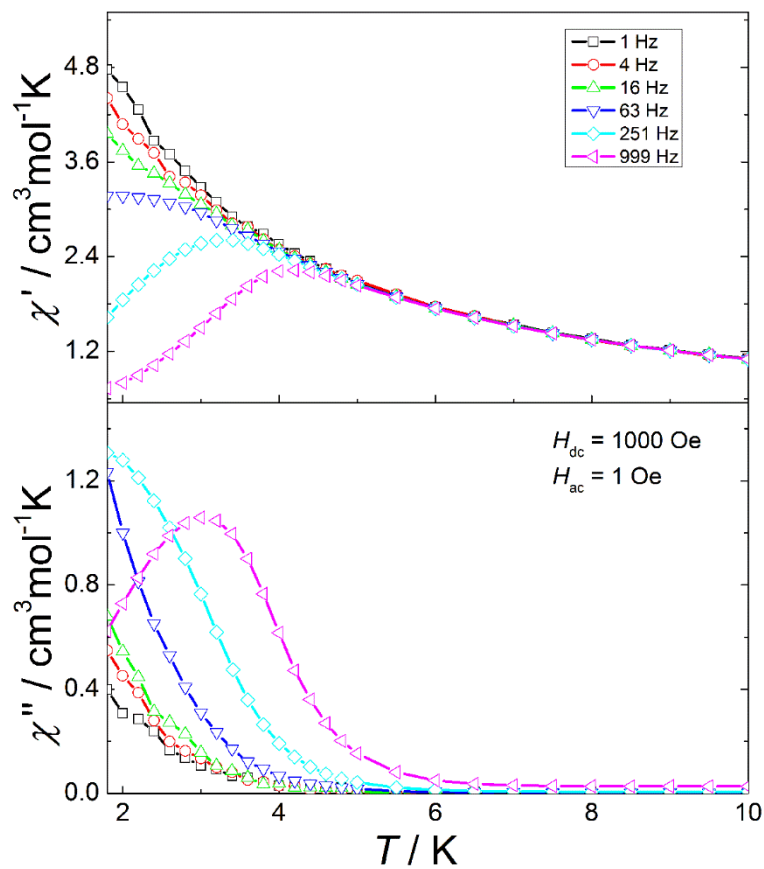


Figure S5. Temperature dependence of the in-phase and out-of-phase ac susceptibility data for **1** under 1000 Oe dc field range from 1.8 to 10 K ($H_{ac} = 1$ Oe). The solid lines are a guide for the eye.

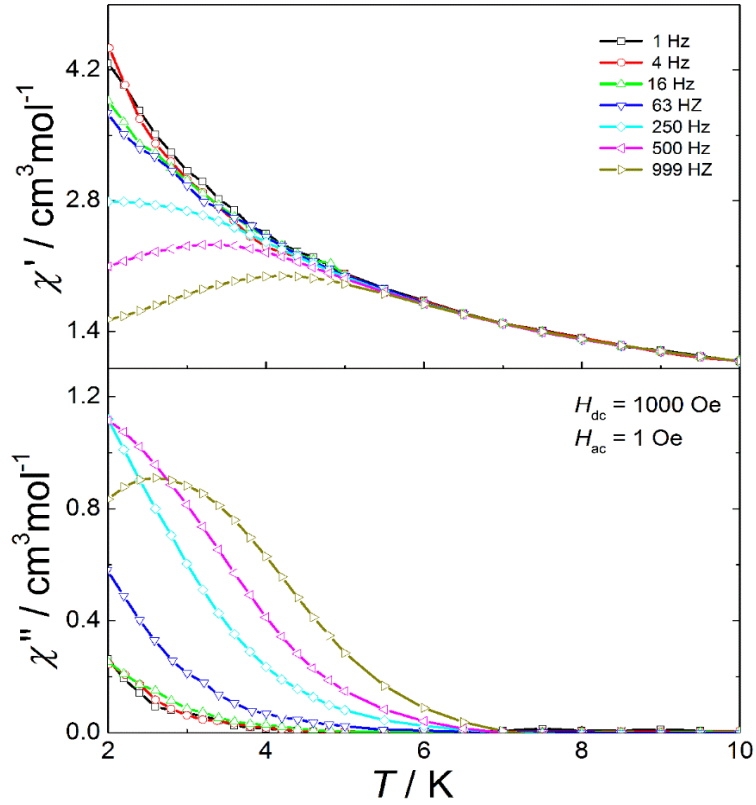


Figure S6. Temperature dependence of the in-phase and out-of-phase ac susceptibility data for **2** under 1000 Oe dc field range from 2 to 10 K ($H_{ac} = 1$ Oe). The solid lines are a guide for the eye.

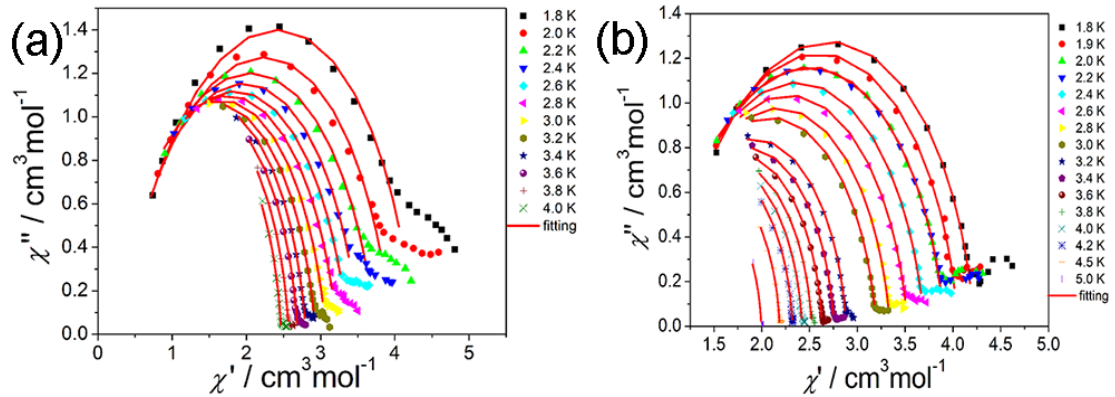


Figure S7. The Cole-Cole plots at 1.8–4.0 K of **1** (a) and at 1.8–5.0 K of **2** (c) measured under 1000 Oe dc field ($H_{ac} = 1$ Oe), and the red solid lines are the best fitting according to the generalized Debye model.

Table S7. Relaxation Fitting Parameters from the Least-Square Fitting of the Cole-Cole plots of **1** according to the Generalized Debye Model.^a

Temperature / K	$\chi_S / \text{cm}^3 \text{mol}^{-1} \text{K}$	$\chi_T / \text{cm}^3 \text{mol}^{-1} \text{K}$	τ / s	α
1.8	0.3007	4.26079	0.00125	0.21613
2.0	0.24872	3.96021	9E-4	0.23388
2.2	0.08	3.75	6.3E-4	0.26204
2.4	0.17654	3.52561	4.8E-4	0.23201
2.6	0.09349	3.37062	3.4E-4	0.23747

2.8	0.05413	3.2255	2.5E-4	0.22901
3.0	0.07196	3.07289	1.9E-4	0.20791
3.2	0.07427	2.93357	1.4E-4	0.18789
3.4	0.09215	2.80117	1E-4	0.15851
3.6	0.12008	2.69382	8E-5	0.14092
3.8	0.15747	2.57161	6E-5	0.11322
4.0	0.15366	2.46967	4E-5	0.09959

^aThe Generalized Debye equation: $\chi'' = (\chi_S - \chi_T) \tanh[\alpha\pi/2]/2 + \{(\chi' - \chi_S)(\chi_T - \chi') + (\chi_T - \chi_S)^2 \tanh^2[\alpha\pi/2]/4\}^{1/2}$ (1), where χ_S is the adiabatic magnetic susceptibility and χ_T is the isothermal magnetic susceptibility; χ' is in-phase susceptibility and χ'' is out-of-phase susceptibility.

Table S8. Relaxation Fitting Parameters from the Least-Square Fitting of the Cole-Cole plots of **2** according to the Generalized Debye Model. ^a

Temperature / K	$\chi_S / \text{cm}^3 \text{mol}^{-1} \text{K}$	$\chi_T / \text{cm}^3 \text{mol}^{-1} \text{K}$	τ / s	α
1.8	1.05191	4.22402	5.9E-4	0.13751
1.9	1.00641	4.0556	5.3E-4	0.13933
2.0	0.91727	3.91552	4.8E-4	0.16110
2.2	0.94394	3.90885	4E-4	0.15365
2.4	0.89640	3.70188	3.3E-4	0.15746
2.6	0.91505	3.52592	2.9E-4	0.14628
2.8	0.90774	3.34191	2.4E-4	0.13855
3.0	0.90059	3.19673	2E-4	0.12951
3.2	0.89943	2.88249	1.7E-4	0.10524
3.4	0.90184	2.75335	1.5E-4	0.09352
3.6	0.88372	2.63081	1.3E-4	0.08295
3.8	0.85160	2.52265	1E-4	0.08740
4.0	0.78402	2.42057	9E-5	0.08155
4.2	0.74374	2.32119	7E-5	0.07072
4.5	0.68980	2.18606	5E-5	0.06711
5.0	0.68457	1.99502	3E-5	0.06768

Reference

- (S1) J. Long, F. Habib, P.-H. Lin, I. Korobkov, G. Enright, L. Ungur, W. Wernsdorfer, L. F. Chibotaru and M. Murugesu, *J. Am. Chem. Soc.*, 2011, **133**, 5319.
- (S2) O. Kahn, *Molecular Magnetism*, VCH Publishers, Inc., New York, 1993, 2.
- (S3) *SAINTE* Version 7.68A, Bruker AXS, Inc.; Madison, WI 2009.
- (S4) G. M. Sheldrick, *SADABS*, Version 2008/1, Bruker AXS, Inc.; Madison, WI 2008.
- (S5) G. M. Sheldrick, *SHELXTL*, Version 6.14, Bruker AXS, Inc.; Madison, WI 2000-2003.